Published in final edited form as:
Circ Res. 2020 August 28; 127(6): 707–723. doi:10.1161/CIRCRESAHA.119.316071.

B55α/PP2A limits endothelial cell apoptosis during vascular remodeling: a complementary approach to kill pathological vessels?

Manuel Ehling[1,2], **Ward Celus**[1,2], **Rosa Martín-Pérez**[1,2], **Roser Alba-Rovira**[1,2,3], **Sander Willox**[1,2], **Giusy Di Conza**[1,2], **Massimiliano Mazzone**[1,2,§]

[1]Laboratory of Tumor Inflammation and Angiogenesis, Center for Cancer Biology (CCB), VIB, Leuven, 3000, Belgium

[2]Laboratory of Tumor Inflammation and Angiogenesis, Department of Oncology, KU Leuven, Leuven, 3000, Belgium.

[3]Vasculitis Research Unit, Department of Autoimmune Diseases, Hospital Clínic, University of Barcelona, Institut dínvestigacions Biomèdiques August Pi I Sunyer (IDIBAPS), Barcelona, Spain.

Abstract

Rationale—How endothelial cells (ECs) migrate and form an immature vascular plexus has been extensively studied. Yet, mechanisms underlying vascular remodeling remain poorly established. A better understanding of these processes may lead to the design of novel therapeutic strategies complementary to those already exploited in the clinic by current angiogenesis inhibitors.

Objective—Starting from our previous observations that the PP2A phosphatase regulates the HIF/PHD2-constituted oxygen machinery, we hypothesized that this axis could play an important role during blood vessel formation and tissue oxygen restoration.

Methods and Results—Here we show that the regulatory PP2A-phosphatase subunit B55α is at the cross-road between vessel pruning and vessel maturation. Blood vessels with high B55α will counter cell stress conditions and thrive for stabilization and maturation. In cases when B55α is inhibited, ECs cannot cope with cell stress and undergo apoptosis, leading to massive pruning of nascent blood vessels which are not yet stabilized and mature.

Mechanistically, we found that the B55α/PP2A complex restrains PHD2 activity, promoting EC survival in a HIF-dependent manner, and furthermore dephosphorylates p38, altogether protecting these cells against cell stress occurring, for example, during the onset of blood flow. In tumors, EC-specific B55α deficiency induces pruning of immature-like tumor blood vessels resulting in

[§]Editorial correspondence to: M. Mazzone: massimiliano.mazzone@kuleuven.vib.be.

Author contributions

M.E. performed the experimental designs, acquisition, analysis and interpretation of all data and wrote the manuscript. W.C. assisted with conducting experiments and writing of the manuscript. R.M.P. designed experiments, performed Co-IPs and WBs and gave scientific input on the biochemistry experiments. R.A.R. performed Co-IP and WBs. S.W. assisted with the *in vivo* experiments and performed immunostainings. G.D.C. initiated the generation of the *Ppp2r2a* KO mice, designed genotyping and qPCR primers and gave scientific input. M.M. performed the experimental designs, conducted scientific direction and wrote the manuscript.

Competing financial interests

No competing financial interests to declare.

Europe PMC Funders Author Manuscripts

delayed tumor growth and metastasis, without affecting non-pathological vessels. Consistently, systemic administration of a pan-PP2A inhibitor disrupts vascular network formation and tumor progression *in vivo* without additional effects on B55α-deficient vessels.

Conclusions—These data underline a unique role of the B55α/PP2A phosphatase complex in vessel remodeling and suggest the use of PP2A-inhibitors as potent anti-angiogenic drugs targeting specifically nascent blood vessels with a mode-of-action that is complementary to currently available VEGF(R)-targeted therapies.

Introduction

Angiogenesis describes a process, by which blood vessels are formed within growing organs or previously avascular tissues. During the initial sprouting phase, activated ECs migrate towards a gradient of secreted growth factors. The fusion of leading tip cells and the start of vessel perfusion then mark the formation of a first vascular network[1]. Albeit being characterized by a high vessel density, this immature plexus is still inefficient and lacks a clear distinction between arteries, capillaries and venous structures[2,3].

To create a mature and stable network, the primitive plexus undergoes several remodeling processes, including the removal of supernumerary capillaries. This process is mediated either by coordinated cell migration or induction of apoptosis[4–6], both of which have to be tightly regulated to avoid inadequate blood flow supply to organs[7].

In contrast to the initial steps of angiogenesis, there is still a tremendous lack of knowledge on mechanisms controlling vascular remodeling and limiting apoptosis-mediated blood vessel pruning, especially in response to cell stress upon the onset of blood flow[8–11]. For example, it is known that HIF-signaling plays a pivotal role in protecting ECs against ROS arising upon vessel perfusion[9,12–14]. Moreover, also the p38 pathway is described to mediate a tightly balanced response to cell stress. While short term activation of p38 induces cell survival and differentiation, mostly *in vitro* data show that also prolonged p38 activation leads to the induction of EC apoptosis[15]. A better understanding of how these remodeling processes are regulated, might present novel therapeutic strategies and intervention points for clinical applications.

So far, research in the angiogenesis field is mainly focusing on VEGF and VEGF receptor families, which are the key mediators of vessel sprouting[16] and vessel maintenance[17]. This focus is also reflected in the clinic, since most of the angiogenesis inhibitors tested so far are agents targeting VEGF or its receptor[18]. However, these drugs prolong the survival of cancer patients without cure and at the expense of severe side effects [19,20]. The combination of current antiangiogenic drugs together with novel agents, which have alternative mechanisms of action, could increase the response and overcome resistance to currently used VEGF-targeted therapies.

In this work, we analyzed the role of the regulatory PP2A phosphatase subunit B55α during vascular development and cancer progression. B55α is one of 26 regulatory subunits which are responsible to orchestrate the activity and substrate specificity of the trimeric PP2A phosphatase complex[21]. We have recently shown that inhibition of B55α in cancer

Europe PMC Funders Author Manuscripts

Europe PMC Funders Author Manuscripts

cells alleviates tumor progression by reducing cell viability in response to hypoxia and glucose starvation[22,23]. However, besides one publication in zebrafish[24], the direct role of B55α in stromal cells remains unknown. Here, we found that genetic deletion of B55α in ECs unleashes apoptosis-mediated blood vessel pruning in the remodeling vascular plexus both during development and cancer progression. Strikingly, not only homozygous but also heterozygous deficiency of B55α is embryonically lethal and demarcated by a severe the collapse of immature vessels. In two different tumor models, we show that genetic loss of B55α in ECs or pharmacologic inhibition of the PP2A phosphatase has a strong anti-angiogenic effect specifically on the abnormal and immature tumor vessels, thereby delaying tumor and metastatic progression.

Methods

EC culture

HUVECs, isolated from human umbilical cords, were cultured in gelatin-coated dishes, using supplemented M199 medium. For dense conditions, $3x10^5$ HUVECs were seeded in the well of a 6-well plate, $3x10^4$ cells were seeded for confluent conditions, $6x10^3$ cells for sparse conditions.

***In vitro* gene silencing—**ShRNA-mediated KD of B55α was performed using three different PLKO lentiviral vectors from Sigma (TRCN0000002489 (shB55α-1); TRCN0000002492 (shB55α-2); TRCN0000002493 (shB55α-3)) and the respective scramble as a control vector.

Chemical inhibitors

Inhibitors were purchased from Sigma or Selleck and, unless indicated otherwise, used in the following concentrations: qVD (50μM), zVAD (100μM), DMOG (1mM), P38 inhibitor (SB203580; 25μM), MnTBAP (100μM), Caspase 8 inhibitor (z-IETD-FMK; 100μM), Necrostatin 1 (30μM), LB100 (2.5μM).

Cell immunostainings and analysis of cell survival

Immunostainings of cultured ECs were done as described before[25].

For the WST1-based cell survival assay (Sigma), $1x10^4$ HUVECs were seeded in a 96-well plate. After treatment, 10% WST-1 solution was added and the absorbance levels, correlating with living cell numbers, were measured and normalized to the respective control group.

RNA and qPCR

Cells were collected in RLT buffer and RNA was isolated using RNeasy Micro- or Mini-kit. Reverse transcription to cDNA was performed using Quantitect Reverse Transcription Kit (Qiagen). RT-PCR was performed as described[26], using commercially available (Applied Biosystems and IDT) or home-made primers and probes.

Western Blots (WBs) and co-immunoprecipitations (Co-IPs)

Protein extraction and WBs were performed as described[22], using antibodies listed in Online Table I. Protein bands were quantified using ImageJ.

Co-IPs were performed in densely cultured HUVECs using Dynabeads protein G. In brief, HUVECs were harvested in lysis buffer (0.025M Tris, 0.15M NaCl, 0.001M EDTA, 1% NP40, 5% glycerol, pH 7.4) and pre-cleaned with uncoated beads. Coated beads were then added to the sample for 4hrs and eluted by adding 50µl of NuPage 1x and boiling at 96°C for 10min.

ROS assay

For ROS-measurements, HUVECs were incubated with CM-H2DCFDA (ThermoFisher Scientific) for 30min in serum free medium. Cells were then washed and the fluorescence (Ex/em 492-495/517-527nm) was measured every 30min before and after exposure to H_2O_2 (50µM). Results were normalized per protein contents.

Generation of *Ppp2r2a*-KO mice

ES cells were obtained by the trans-NIH Knock-Out Mouse Project (KOMP). The neo-cassette and exon 6 was removed by intercrossing these mice with Pgk1.Cre[27] deleter mice, generating global KO mice (Online Fig. I F). The correct recombination was verified on the genomic DNA; B55α depletion was then confirmed on RNA and protein levels.

To generate conditional KO mice, we intercrossed mice with the original construct to FLPeR[28] mice (Online Fig. I F). The resulting *Ppp2r2a*-loxed mice were then crossed to LysM.Cre[29], Rosa26.iCre[30], VEcad.iCre[31] and Prox1.iCre[32] deleter lines.

Gene deletion using tamoxifen was induced as described previously[2]. Deletion efficiency was confirmed by qPCR. All experiments were conducted in a C57BL/6 background using littermate controls. Housing and experimental animal procedures were approved by the Institutional Animal Care and Research Advisory Committee of the KU Leuven.

FACS-sorted EC

Murine lungs or embryonic tissues were dissected, mechanically dissociated and digested using collagenase I/II and dispase. Cell suspensions were stained using antibodies in Online Table I. Viable $CD45^-$, $CD31^+$, $Pdpn^-$ vascular ECs and $CD45^-$, $CD31^+$, $Pdpn^+$ lymphatic ECs were sorted by FACS Aria (BD Bioscience) and stored in RLT buffer.

Tumors and sponge assays

Murine Lewis lung (LLC) and E0771 breast adenocarcinoma cells were obtained from the American Type Cultures Collection (ATCC). $1x10^6$ LLC cells were injected subcutaneously while $5x10^5$ E0771 cells orthotopically in the mammary fat pad. Tumor size was monitored throughout the whole experiment. At endpoint, tumor weight was measured and superficial lung metastatic nodules were quantified under a stereomicroscope. Tumors were harvested and fixed in 2% formaldehyde o/n before being processed for histology.

For resection experiments, tumors with an average size of 700mm^3 were surgically removed. After recovery, deletion of B55α was induced by daily administration of tamoxifen for 5 days. At the end stage, lungs were dissected and weighed as a readout for the metastatic burden. After fixation in 2% formaldehyde o/n, paraffin sections were prepared and processed for H&E staining and immunostainings.

To measure cancer cell extravasation, 0.5x10^6 LLCs, stably transduced with a CMV promoter in a lentivector, were injected into the tail vein of control and B55α$^{iEC\text{-}KO}$ mice. After 96hrs lungs were harvested and CMV-positive LLCs were quantified by qPCR.

The sponge-implantation angiogenesis assay was performed as described previously[33]. After ex vivo treatment with 25µl of LLC tumor-conditioned media, serving as an initial attractor for blood vessel formation, 4 sponges were subcutaneously implanted on the ventral side of each animal. Three days after implantation, we started the treatments by injections of 25µl of the indicated inhibitors such as the Phd inhibitor DMOG (2mM), the P38 inhibitor SB203580 (low dose = 12.5µM; high dose = 100µM) or the PP2A inhibitor LB100 (low dose= 1µM; high dose=2.5µM dose) into the center of the implanted sponge every 48 hours. Sponges within the same animal but treated with the according solvent only (e.g. PBS) served as negative control. Ten days after implantation, the sponges were harvested and stored in OCT at -80°C. In order to analyze the morphology and density of blood vessels within these sponges, we performed CryoSections and immunostainings for CD31 and Hoechst.

Histology and immunostainings

Immunostainings of whole mount skin and retina samples were performed as described previously[2]. Healthy organs, metastasis bearing lungs and tumor sections were fixed in 2% PFA o/n at 4°C, dehydrated and embedded in paraffin. 7µm-thick sections were stained in H&E and immunostained as previously described[34] using antibodies listed in Online Table I.

To visualize tumor blood vessels, 80µm-thick cryosections were stained for CD31, clCasp3 and Hoechst. Tumor hypoxia was analyzed by i.p. injection of pimonidazole hydrochloride 2hrs prior to dissection followed by immunostainings with Hypoxyprobe-1-Mab1 (Hypoxyprobe kit, Chemicon). Microscopic analysis and quantifications were done with an Olympus BX41 microscope and CellSense software.

RNAscope

Sections of 4µm of thickness were obtained from paraffin-embedded tissues. RNAscope 2.5 HD Detection Kit (ACD, Cat No. 322350) was used with the RNAscope Probe Mm-Ppp2r2a (ACD, Cat No. 549391) according to the manufacturer's protocol followed by immunostainings for CD31. Images were acquired on the Zeiss Axio Scan.Z1 using a x40 objective and ZEN2 software.

Statistical analysis

Statistical analysis was performed using GraphPad Prism software and significance calculated by two-tailored t-test or two-way ANOVA respectively. Mathematical outliers

were detected using Grubbs test in GraphPad. Independent experiments were pooled and analyzed together whenever possible.

Results

B55α is a key regulator of vascular remodeling during embryonic development

Although the different regulatory B-subunits of the PP2A phosphatase complex have been suggested to have partially redundant functions, we found a conservation rate of 100% between human and murine B55α protein (Fig. 1A), pointing to a unique role of this regulatory subunit. We then decided to analyze *in vivo* the expression pattern of *Ppp2r2a* (the gene codifying for B55α) by using RNAscope. In mouse embryos, B55α was expressed by several cell types and especially $CD31^+$ blood vessels (Fig. 1B). In adult mice, expression of B55α in the quiescent vasculature was strongly diminished if not absent, while markedly detectable in sites of active angiogenesis as it occurs in progressing tumors (Online Fig. I A-E). These data point towards the hypothesis that B55α is required at some step during the formation of the vascular plexus while it is not necessary in a quiescent and mature vasculature (as it is the case in adults).

To analyze the functional role of B55α, we firstly generated embryos with homo- and heterozygous deletion for the *Ppp2r2a* gene (Online Fig. I F). Deletion efficiency was confirmed at embryonic stage E12.5 on RNA and protein levels (Fig. 1D-F). In line with the high conservation rate, *Ppp2r2a* gene deletion led to embryonic lethality around E14.5 (Fig. 1C). The fact that not only homozygous, but also more than 50% of heterozygous knockout (KO) embryos died during development underline the importance of B55α in embryogenesis. However, surviving adult heterozygous mice were fertile and did not show any obvious defects. Embryonic lethality was accompanied by strong defects in remodeling blood vessels (Fig. 1H-K), but not in the initially formed immature vascular plexus (Online Fig. I H,I). In addition to the vascular defects, mutant embryos also displayed aberrant lymphatic vessel structures (Fig. 1L,M).

In order to analyze the selective role of B55α in ECs, *Ppp2r2a(lox/lox)* conditional KO mice were intercrossed with the VEcadherin.CreERT2 strain (henceforward $B55\alpha^{iEC\text{-}KO}$) allowing for tamoxifen-induced deletion of B55α in ECs (Online Fig. I F). In line with the results in Full-KO embryos, we found that genetic deletion of B55α in ECs did not lead to any obvious defects during the initial steps of blood vessel formation neither in embryonic skin nor in postnatal retina samples (Online Fig. II A-F). However, lack of endothelial B55α had a severe impact on vascular and lymphatic vessel structures in regions of vascular remodeling (Fig. 2A-F). Moreover, endothelial B55α deletion drastically increased the density of cleaved $Caspase\text{-}3^+$ ECs in mutant embryos (Fig. 2G,I) and in the remodeling vasculature of retina samples (Online Fig. II G-K), which led to increased blood vessel pruning during vascular remodeling (Fig. 2H,J). In general, the induction of cleaved Caspase-3 preceded the general collapse of blood vessels in less remodeled areas of the vascular plexus (Online Fig. II C,D), suggesting that EC apoptosis was the cause rather than the consequence of blood vessel pruning. As a result of the severe and progressing vascular defects, EC-specific deletion of B55α led to embryonic lethality by E16.5 (Fig. 2K-O).

Similar to the defects observed in full KO embryos (Fig. 1L,M), EC-specific deletion of B55α also resulted in enlarged and activated lymph vessels in embryonic skin samples (Fig. 2C,E,L,O). In contrast, *Ppp2r2a* deletion selectively in LECs (via the intercross of floxed mice with the LEC-specific Prox1.CreERT2 deleter strain) did not recapitulate these lymphatic defects (Online Fig. III D-I). The lymphatic phenotype in B55α$^{iEC\text{-}KO}$ embryos might be explained by the fact that deletion of B55α in vascular ECs caused excessive blood vessel pruning. This, together with the resulting hypoxic microenvironment can affect lymphatic network formation indirectly[35] and thus induce lymphatic aberrations as observed in pan-EC KO mice.

Overall, these data indicate that B55α has a very specific and unique role in the formation of a blood vessel network but is dispensable in LECs.

Lack of endothelial B55α delays tumor progression

In contrast to the severe effects observed during development, neither EC-specific nor ubiquitous deletion (using Rosa26.CreERT2 mice) of *Ppp2r2a* led to lethality or any overt organ defects when initiated in 8-10 weeks old adult mice (Online Fig. IV A-K). In addition, also histological analysis of different organs from adult B55α$^{iEC\text{-}KO}$ mice did not reveal any vascular or lymphatic defects (Online Fig. IV F-W). This is consistent with the fact that *Ppp2r2a* expression is downregulated in quiescent blood vessels of fully mature organs in adult mice (Online Fig. I A-C) and supports the idea that B55α plays a crucial role only during blood vessel remodeling while it is dispensable for the maintenance of vessel quiescence.

Since tumor blood vessels are mostly immature[36] and express high levels of *Ppp2r2a* (Online Fig. I D,E), we wondered whether B55α inhibition would induce pruning of these aberrant vessels, similar to the effects we observed during development. Therefore, we injected either LLC cells subcutaneously or E0771 breast cancer cells orthotopically in tamoxifen-treated control and B55α$^{iEC\text{-}KO}$ mice. We observed that EC-specific deletion of B55α (Online Fig. IV D) resulted in a strongly delayed tumor progression and metastasis formation in both models when compared to controls (Fig. 3A,D). Furthermore, the decrease in tumor size and weight (Fig. 3B,E) was accompanied with enhanced tumor hypoxia and necrosis (Fig. 3G-N). At the same time, we observed that also lung metastasis were reduced in mutant mice (Fig. 3C,F). However, tumor cell extravasation was not directly altered by lack of endothelial B55α (Online Fig. V B).

Although we did not find any defects in the vasculature of healthy organs, tumor blood vessels of mutant mice had an altered shape, were less dense and less well connected when compared to controls (Fig. 3O-S,V). In addition, and reminiscent to the effects found during development, lack of B55α led to an increased number of apoptotic ECs within the tumor vasculature (Fig. 3S,U,V,X). However, this effect was restricted to immature and nascent blood vessels, since the vascular density in adult organs did not changed upon loss of endothelial B55α (Online Fig. IV F,G,L-W).

Induction of B55α deletion following tumor resection inhibits metastatic growth and prolongs survival

Our results in cancer cells[22,23] and the current data in ECs suggest that pharmacologic inhibition of B55α/PP2A might represent an interesting approach in cancer therapy. However, most clinical treatments only start after the main tumor is detected and surgically resected. These approaches aim to inhibit metastasis progression, which account for the majority of cancer related deaths[37].

To mimic this clinical setting, we injected wildtype LLC cancer cells in mice which were not yet treated with tamoxifen (Fig. 4A). In line with the non-recombined *Ppp2r2a* gene, tumors in these mice progressed identical (Fig. 4B). Tumors were then surgically removed at an average size of 700 mm^3 and 3 days later tamoxifen treatment was initiated in order to induce EC-specific *Ppp2r2a* deletion. As compared to control mice, EC-specific *Ppp2r2a* deletion conferred a longer survival and a drastic reduction in lung metastasis (Fig. 4C-H). Albeit having similar numbers of lung metastasis (Fig. 4D), lack of endothelial B55α led to a delayed progression and reduced growth of these metastatic lesions (Fig. 4E-H). Similar to the effects observed in primary tumors, blood vessel density within the angiogenic active metastatic site was strongly impaired (Fig. 4I-J).

Chemical inhibition of the PP2A phosphatase induces blood vessel pruning and delays tumor progression *in vivo*

Although specific inhibitors for the B55α/PP2A are not currently available yet, the pan-PP2A inhibitor LB100 was recently approved in a clinical phase 1 study for use in human patients with 2 additional Phase II clinical trials still ongoing[38–40].

In order to test whether LB100-mediated chemical inhibition of PP2A had an anti-angiogenic effect, without affecting cancer or stromal cells directly, we conceived experiments where sponges conditioned with tumor-conditioned medium were used to monitor angiogenesis (Fig. 5A)[33]. Even at a low dose, LB100 was able to disrupt the immature vascular network formation in sponges of WT mice but did not achieve any further effect in $B55\alpha^{iEC\text{-}KO}$ mice (Fig. 5B,C). Encouraged by these results, we then analyzed the effects of low dose LB100 treatment on tumor progression. We found that daily administration of LB100 reduced LLC tumor growth down to a similar extent as in $B55\alpha^{iEC\text{-}KO}$ (Fig. 5D,E) without showing any overt signs of toxicity (Fig. 5F). In addition, also the reduction in tumor vessel density was comparable in both $B55\alpha^{iEC\text{-}KO}$ and LB100 treated mice (Fig. 5G,H), resulting in increased tumor hypoxia under both conditions (Fig. 5I,J). As in $B55\alpha^{iEC\text{-}KO}$ mice, LB100-treated tumors did not alter the ratio of pericyte-covered tumor blood vessels (Online Fig. V C). Overall, these data provide a proof-of-principle that PP2A inhibitors have a potent apoptosis inducing effect on immature vessels, which is mediated by the B55α/PP2A complex expressed in ECs.

B55α deficiency induces apoptosis in maturating ECs but not in other cell types

We then set up a model to study the role of B55α on EC apoptosis *in vitro*. As a cell system, we used HUVECs seeded in growth factor supplemented medium, either sparse or densely seeded. As used by several others[41,42], this is a simplified system comparing

proliferative *versus* non-proliferative angiogenic ECs, the latter resembling two features that characterize the endothelial lining of remodeling blood vessels *i.e.*, cell contact inhibition and the exposure to a cytokine and growth factor surge.

We found that B55α was upregulated in densely-seeded ECs at both mRNA and protein levels when compared to sparse ECs (Fig. 6A,B). Similar to the *in vivo* results, lentivirus-mediated shRNA knockdown (KD) of B55α led to a drastic decrease of EC numbers specifically in dense HUVECs (Fig. 6C, Online Fig. VI B,C), which was mediated by apoptosis induction in KD-ECs (Fig. 6D-H). Furthermore, treatment with the pan-Caspase inhibitors zVAD as well as qVD (Fig. 6F-H), but neither with the necroptosis inhibitor Nec1 nor with an Caspase8 inhibitor (a mediator of the extrinsic apoptotic pathway) rescued EC survival (Online Fig. VI E,F). Taken together, these data suggest that B55α loss leads to an activation of the intrinsic apoptotic pathway in vascular ECs.

The apoptotic effect observed upon genetic silencing of B55α, and recapitulated by using the PP2A pan-inhibitor LB100 was far less pronounced in proliferating, sparse HUVECs (Fig. 6I-L) and restricted to vascular ECs, as PP2A inhibition in other cell types, such as different cancer cell lines, macrophages or even LECs did not induce apoptosis (Online Fig. VI D; Online Fig. III B,J,K). These data suggest that PP2A masters an anti-apoptotic program which is crucial for the survival of neoformed endothelia but not of proliferating ECs or other cell types.

B55α counteracts ROS in a PHD/HIF dependent manner

We then studied the mechanism through which B55α loss could induce EC apoptosis in the neoformed vessels of the remodeling vascular plexus. Given the involvement of PHD2/HIF in vessel remodeling[22,43] and ROS scavenging[9,12–14], as well as our previous work showing a B55α-mediated regulation of PHD2 activity and vice versa[22,23], we initially focused on this signaling axis. When HUVECs were grown from sparse to dense in the presence of MnTBAP, a well-characterized ROS-scavenging molecule[44,45], protein upregulation of B55α was strongly prevented (Fig. 7A). Furthermore, only non-proliferative ECs cultured under dense conditions were protected against H_2O_2 induced ROS-stress in a B55α-dependent manner (Fig. 7B,C). In line with our work in cancer cells, B55α accumulation in dense HUVECs allowed HIF1α and HIF2α stabilization even under normoxia, while protein levels of HIF1/2α were strongly reduced upon B55α-KD (Fig. 7D). Treatment with the PHD2 inhibitor DMOG reversed this effect in B55α-KD HUVECs and led to a reduction in cell stress, indicated by reduced levels of phospho-eIF2α and p21 (Fig. 7E).

Interestingly, sparse HUVECs upregulated B55α already after exposure to low doses of H_2O_2 (50μM), which had no effect on ROS-protected, dense ECs (Fig. 7F). In contrast, exposure to high doses of H_2O_2, (500μM), which was lethal for sparse HUVECs, led to further upregulation of B55α in dense HUVECs. This supports the idea that ECs upregulate B55α in order to counteract otherwise lethal levels of ROS. In addition, DMOG treatment in B55α-KD HUVECs (Fig. 7G) restored the expression of ROS-scavenging genes back to the levels measured in B55α-proficient HUVECs (Fig. 7H-K). As a consequence, DMOG-treated B55α-KD HUVECs showed a restored capacity to counteract ROS and a partial but

significant rescue in cell survival (Fig. 7N-P). These results suggest that B55α/PP2A elicits a HIF-mediated anti-oxidative program via PHD2 inhibition[22].

To show whether this signaling axis had a relevance *in vivo* directly on ECs without having a bias interpretation due to the indirect response of cancer or tumor stroma cells, we performed sponge assays in control and B55α^{iEC-KO} mice. In line with our *in vitro* results, sponges implanted in B55α^{iEC-KO} mice had very few blood vessels, but DMOG treatment led to a significant rescue (Fig. 7Q,R).

Though DMOG is a non-specific PHD2 inhibitor, based also on our previous findings[22,23] we can speculate that B55α is upregulated in non-proliferative ECs of the neoformed vascular plexus in order to inhibit PHD2 and allow a HIF-mediated response that protects the nascent endothelium against oxidative stress, a condition linked to the onset of blood flow[9,12–14]

B55α/PP2A modulates a cell stress response by dephosphorylating p-p38

Given that DMOG treatment only partially improved the survival of ECs lacking B55α both *in vitro* and *in vivo*, we speculated that an additional B55α dependent signaling axis was involved in the regulation of EC apoptosis. We found that p38 phosphorylation in B55α-KD HUVECs was higher than in control cells (Fig. 8A), an effect persistent after inhibition of PHD2 (Fig. 7E). We hypothesized that B55α/PP2A might be able to regulate p38 signaling either directly or indirectly by modulating upstream activators such as AMPK and PKR[15,46,47]. By performing co-immunoprecipitation experiments we found a direct binding of B55α to p38 (Fig. 8B), but no interaction with AMPK or PKR (Online Fig. VI H) in samples derived from densely seeded HUVECs.

In line with previous findings, showing that prolonged phosphorylation and thus hyper-activation of p38 results in EC apoptosis[15], chemical inhibition of p38 improved survival in B55α-KD ECs by normalizing p38 activity levels in these cells (Fig. 8C-E). In contrast, acute pharmacological blockade of p38 promoted cell death in control ECs. This could be explained by the fact that also too low levels of p38 activation induces apoptosis in ECs (Fig. 8E)[15].

To assess if prolonged activation of p38 after B55α deletion played a role for our phenotype *in vivo*, we used again the sponge implantation model. In line with our *in vitro* data, chemical inhibition of p38 led to a dose dependent rescue of blood vessel density in B55α^{iEC-KO} mice while having the opposite effect in control mice (Fig. 8G-H). This supported the idea that p38 activity, precisely controlled by the B55α/PP2A phosphatase, is crucial for optimal blood vessel formation also *in vivo*.

Discussion

Early publications dealing with vascular remodeling often described blood vessel pruning as angiogenesis occurring in reverse. In this scenario, the onset of blood flow would cause a withdrawal of pro-angiogenic survival factors, leading to an apoptosis mediated removal of abundant ECs[11,48]. However, in order to generate a highly effective and functional network,

a plethora of well-coordinated processes are occurring at the same time and have to be tightly regulated. Although some of these pathways might be shared with early angiogenic processes, additional and yet unidentified molecular regulators might be important at later stages only. In contrast to the early steps of angiogenesis, these later remodeling processes are only poorly understood.

In this work, we genetically deleted B55α in ECs and found that, while B55α is dispensable for initial vessel formation, it plays a major role in the remodeling vasculature. Consistently, genetic deletion of B55α led to enhanced EC apoptosis within the remodeling plexus and thus to a drastic pruning of the initially formed but still immature vasculature. Interestingly, chemical pan-PP2A inhibition had no additional effects on blood vessel pruning in B55α$^{iEC\text{-}KO}$ mice, suggesting that these signaling pathways and vascular remodeling are mainly regulated by the B55α/PP2A holocomplex but not any of the other 26 regulatory subunits.

Our findings imply that B55α is upregulated at the late stages of vessel formation when some of the newly formed vessels will undergo maturation while others undergo pruning, overall increasing the efficiency of the vascular network and thus tissue perfusion. Thereby, expression of B55α allows immature blood vessels to undergo the way of maturation while ECs lacking B55α would be unprotected against cell stress, especially after the start of blood flow or in the harsh tumor microenvironment. As a result, deletion of B55α leads to a less dense vascular network by inducing EC apoptosis and hyperpruning of nascent blood vessels. However, lack of B55α did not affect early angiogenic processes such as angiogenic sprouting or fully mature blood vessels. The upstream regulation of B55α during angiogenic blood vessel remodeling has been recently ascribed to the engagement of endothelial integrin α5β1 which, upon binding to fibronectin, would favor the formation and stabilization of a B55α/PP2A complex[49].

The role of B55α in the remodeling vasculature is supported by another publication, showing a similar phenotype in developing zebrafish embryos[24]. However, this previous study suggests that EC apoptosis might be secondary to a diminished blood flow following blood vessel collapse[50]. In contrast, the combination of our *in vitro* and *in vivo* data show that EC apoptosis in the remodeling blood vessels upon B55α deletion occurs independent of and even precedes the retraction of immature blood vessels. The lack of sprouting defects and identical vessel densities in the immature vascular plexus also suggest that ECs did not just become less responsive to angiogenic stimuli *per se*. In contrast, B55α has a very specific role in restricting EC-apoptosis during vascular remodeling.

Since the onset of blood flow leads to a strong burst of ROS, ECs in the immature plexus have to find a way to counteract this cell stress. Previous publications from us and other labs showed an interaction between B55α and PHD2/HIF, which can counteract ROS-mediated cell stress, so we first focused on this signaling axis[9,10,12–14]. We found that B55α expression in dense HUVECs indeed allowed for the engagement of a vasoprotective HIF[12,51] signaling that leads to the upregulation of genes counteracting ROS.

However, inhibition of PHD2 using DMOG only led to a partial rescue in B55α-KD ECs *in vitro* and *in vivo*, thus implying the involvement of PHD2-independent mechanisms in

the regulation of EC survival by B55α. It is known that also a proper balance of p38 activation is crucial for EC survival under cell stress conditions, such as the onset of blood flow[15]. Complete loss of p38 is embryonically lethal due to defects in placental blood vessel formation[52]. However, also overactivation of p38 induces EC apoptosis, as was mainly shown *in vitro*[15,53]. Taken together, these data suggest that the proper balance of p38 activity is crucial to ensure EC survival under cell stress conditions. Our data suggest that B55α/PP2A maintains this fine balance by dephosphorylating p38, resulting in normalized levels of p38 activation. Initial activation of p38 can be triggered by multiple stimuli such as cell stress or growth factors[54]. Therefore, in our settings, initial p38 phosphorylation might slightly differ *in vivo* and *in vitro*. As an example, HUVEC medium contains plenty of cytokines and growth factors which can activate p38 signaling. Unlikely, in perfused blood vessel elevated levels of oxygen and physical cell stress might play the major role in inducing p38 activation.

Although, we cannot fully exclude that, besides p38 and PHD2, B55α/PP2A could fine-tune EC survival in remodeling blood vessels by dephosphorylating additional substrates[49] our rescue experiments *in vivo* strongly support the idea that p38 and PHD2 are the main targets in this context.

From a therapeutic point-of-view, our data show that both genetic deletion of B55α and a pan-PP2A phosphatase inhibitor hinder primary tumor growth by inducing EC apoptosis in the most immature blood vessels. Furthermore, genetic deletion of B55α reduced the metastatic burden and extended survival in a model of metachronous disease *i.e.* a metastatic relapse in the absence of primary tumor. Finally, of the two cancer models tested, namely E0771 and LLC tumors, the latter is known to be unresponsive to traditional anti-angiogenic therapies such as VEGF(R) inhibitors[55,56]. Altogether, these data pave the way for the design of B55α/PP2A blockers and suggest their use as single agents or in combination with VEGF-targeted therapies to overcome resistance in cancer treatment. The observations that B55α was not detectable in fully mature, stabilized blood vessels of adult organs, and that mural cell-covered tumor blood vessels were still detectable in B55α$^{iEC\text{-}KO}$ (or LB100-treated) mice, lead to additional clinical speculations. Firstly, B55α/PP2A blockers or pan-PP2A inhibitors affect only remodeling blood vessels whereas VEGF(R) inhibitors mainly target hyperactive ECs. Yet, B55α/PP2A blockers or pan-PP2A inhibitors would spare mature vessels. In tumors, mature and “normalized” vessels are the routes for anti-cancer drugs (such as chemotherapy) to get into the tumor[12]. In healthy organs, disturbance of blood vessel homeostasis causes severe side effects[17] as observed in the clinical use of anti-VEGF(R) drugs[20,36,57]. Thus, B55α/PP2A inhibition can be complementary to VEGF-targeted therapies, but tackle pathological blood vessels more selectively than current antiangiogenic drugs.

In summary, by gaining a mechanistic understanding of processes controlling blood vessel remodeling and maturation we were able to identify a novel and yet unexplored target for multiple clinical interventions[58].

Europe PMC Funders Author Manuscripts

Acknowledgements

We thank Tanja Rothgangl, Federica Diofano, Lena Burchhart, Jens Serneels, Sarah Trusso and Eline Achten for excellent technical help and assistance.

M.E. was supported by the Deutsche Forschungsgemeinschaft (EH 472/1-1) and Kom op tegen Kanker (Stand up to Cancer), the Flemish cancer society (2016/10538/2453). W.C. by an FWO-Strategic Basis Research (SB) doctoral fellowship (1S26917N), R.M.P. by FWO, R.A.R. by FPI associated to SAF 2017/88275-R and G.D.C. by an Pegasus FWO-Marie Curie fellowship (12114113N). M.M. received an ERC consolidator grant (773208) and FWO (G0D1717N) project grant.

References

1. Adams RH, Alitalo K. Molecular regulation of angiogenesis and lymphangiogenesis. Nat Rev Mol Cell Biol. 2007; 8: 464–478. DOI: 10.1038/nrm2183 [PubMed: 17522591]
2. Ehling M, Adams S, Benedito R, Adams RH. Notch controls retinal blood vessel maturation and quiescence. Development. 2013; 140: 3051–3061. DOI: 10.1242/dev.093351 [PubMed: 23785053]
3. Mukouyama YS, Shin D, Britsch S, Taniguchi M, Anderson DJ. Sensory nerves determine the pattern of arterial differentiation and blood vessel branching in the skin. Cell. 2002; 109: 693–705. [PubMed: 12086669]
4. Watson EC, et al. Apoptosis regulates endothelial cell number and capillary vessel diameter but not vessel regression during retinal angiogenesis. Development. 2016; 143: 2973–2982. DOI: 10.1242/dev.137513 [PubMed: 27471260]
5. Franco CA, et al. Dynamic endothelial cell rearrangements drive developmental vessel regression. PLoS Biol. 2015; 13 e1002125 doi: 10.1371/journal.pbio.1002125 [PubMed: 25884288]
6. Xu C, et al. Arteries are formed by vein-derived endothelial tip cells. Nat Commun. 2014; 5 5758 doi: 10.1038/ncomms6758 [PubMed: 25502622]
7. Carmeliet P. Angiogenesis in health and disease. Nat Med. 2003; 9: 653–660. DOI: 10.1038/nm0603-653 [PubMed: 12778163]
8. Baeyens N, Bandyopadhyay C, Coon BG, Yun S, Schwartz MA. Endothelial fluid shear stress sensing in vascular health and disease. J Clin Invest. 2016; 126: 821–828. DOI: 10.1172/JCI83083 [PubMed: 26928035]
9. Staiculescu MC, Foote C, Meininger GA, Martinez-Lemus LA. The role of reactive oxygen species in microvascular remodeling. Int J Mol Sci. 2014; 15: 23792–23835. DOI: 10.3390/ijms151223792 [PubMed: 25535075]
10. Santoro MM. Fashioning blood vessels by ROS signalling and metabolism. Semin Cell Dev Biol. 2018; 80: 35–42. DOI: 10.1016/j.semcdb.2017.08.002 [PubMed: 28800930]
11. Korn C, Augustin HG. Mechanisms of Vessel Pruning and Regression. Dev Cell. 2015; 34: 5–17. DOI: 10.1016/j.devcel.2015.06.004 [PubMed: 26151903]
12. Leite de Oliveira R, et al. Gene-targeting of Phd2 improves tumor response to chemotherapy and prevents side-toxicity. Cancer Cell. 2012; 22: 263–277. DOI: 10.1016/j.ccr.2012.06.028 [PubMed: 22897855]
13. Kapitsinou PP, et al. Endothelial HIF-2 mediates protection and recovery from ischemic kidney injury. J Clin Invest. 2014; 124: 2396–2409. DOI: 10.1172/JCI69073 [PubMed: 24789906]
14. Scortegagna M, et al. Multiple organ pathology, metabolic abnormalities and impaired homeostasis of reactive oxygen species in Epas1-/- mice. Nat Genet. 2003; 35: 331–340. DOI: 10.1038/ng1266 [PubMed: 14608355]
15. Corre I, Paris F, Huot J. The p38 pathway, a major pleiotropic cascade that transduces stress and metastatic signals in endothelial cells. Oncotarget. 2017; 8: 55684–55714. DOI: 10.18632/oncotarget.18264 [PubMed: 28903453]
16. Ferrara N, Gerber HP, LeCouter J. The biology of VEGF and its receptors. Nat Med. 2003; 9: 669–676. DOI: 10.1038/nm0603-669 [PubMed: 12778165]
17. Lee S, et al. Autocrine VEGF signaling is required for vascular homeostasis. Cell. 2007; 130: 691–703. DOI: 10.1016/j.cell.2007.06.054 [PubMed: 17719546]

Europe PMC Funders Author Manuscripts

18. Ribatti D, Annese T, Ruggieri S, Tamma R, Crivellato E. Limitations of Anti-Angiogenic Treatment of Tumors. Transl Oncol. 2019; 12: 981–986. DOI: 10.1016/j.tranon.2019.04.022 [PubMed: 31121490]
19. Hurwitz H, et al. Bevacizumab plus irinotecan, fluorouracil, and leucovorin for metastatic colorectal cancer. N Engl J Med. 2004; 350: 2335–2342. DOI: 10.1056/NEJMoa032691 [PubMed: 15175435]
20. Loges S, Mazzone M, Hohensinner P, Carmeliet P. Silencing or fueling metastasis with VEGF inhibitors: antiangiogenesis revisited. Cancer Cell. 2009; 15: 167–170. DOI: 10.1016/j.ccr.2009.02.007 [PubMed: 19249675]
21. Eichhorn PJ, Creyghton MP, Bernards R. Protein phosphatase 2A regulatory subunits and cancer. Biochim Biophys Acta. 2009; 1795: 1–15. DOI: 10.1016/j.bbcan.2008.05.005 [PubMed: 18588945]
22. Di Conza G, et al. The mTOR and PP2A Pathways Regulate PHD2 Phosphorylation to Fine-Tune HIF1alpha Levels and Colorectal Cancer Cell Survival under Hypoxia. Cell Rep. 2017; 18: 1699–1712. DOI: 10.1016/j.celrep.2017.01.051 [PubMed: 28199842]
23. Di Conza G, Trusso Cafarello S, Zheng X, Zhang Q, Mazzone M. PHD2 Targeting Overcomes Breast Cancer Cell Death upon Glucose Starvation in a PP2A/B55alpha-Mediated Manner. Cell Rep. 2017; 18: 2836–2844. DOI: 10.1016/j.celrep.2017.02.081 [PubMed: 28329677]
24. Martin M, et al. PP2A regulatory subunit Balpha controls endothelial contractility and vessel lumen integrity via regulation of HDAC7. EMBO J. 2013; 32: 2491–2503. DOI: 10.1038/emboj.2013.187 [PubMed: 23955003]
25. Cao J, et al. Polarized actin and VE-cadherin dynamics regulate junctional remodelling and cell migration during sprouting angiogenesis. Nat Commun. 2017; 8 2210 doi: 10.1038/s41467-017-02373-8 [PubMed: 29263363]
26. Fischer C, et al. Anti-PlGF inhibits growth of VEGF(R)-inhibitor-resistant tumors without affecting healthy vessels. Cell. 2007; 131: 463–475. DOI: 10.1016/j.cell.2007.08.038 [PubMed: 17981115]
27. Lallemand Y, Luria V, Haffner-Krausz R, Lonai P. Maternally expressed PGK-Cre transgene as a tool for early and uniform activation of the Cre site-specific recombinase. Transgenic Res. 1998; 7: 105–112. [PubMed: 9608738]
28. Farley FW, Soriano P, Steffen LS, Dymecki SM. Widespread recombinase expression using FLPeR (flipper) mice. Genesis. 2000; 28: 106–110. [PubMed: 11105051]
29. Clausen BE, Burkhardt C, Reith W, Renkawitz R, Forster I. Conditional gene targeting in macrophages and granulocytes using LysMcre mice. Transgenic Res. 1999; 8: 265–277. [PubMed: 10621974]
30. Jullien N, et al. Use of ERT2-iCre-ERT2 for conditional transgenesis. Genesis. 2008; 46: 193–199. DOI: 10.1002/dvg.20383 [PubMed: 18395834]
31. Wang Y, et al. Ephrin-B2 controls VEGF-induced angiogenesis and lymphangiogenesis. Nature. 2010; 465: 483–486. DOI: 10.1038/nature09002 [PubMed: 20445537]
32. Bazigou E, et al. Integrin-alpha9 is required for fibronectin matrix assembly during lymphatic valve morphogenesis. Dev Cell. 2009; 17: 175–186. DOI: 10.1016/j.devcel.2009.06.017 [PubMed: 19686679]
33. Deskins DL, Ardestani S, Young PP. The polyvinyl alcohol sponge model implantation. J Vis Exp. 2012; doi: 10.3791/3885
34. Wenes M, et al. Macrophage Metabolism Controls Tumor Blood Vessel Morphogenesis and Metastasis. Cell Metab. 2016; 24: 701–715. DOI: 10.1016/j.cmet.2016.09.008 [PubMed: 27773694]
35. Schulte-Merker S, Sabine A, Petrova TV. Lymphatic vascular morphogenesis in development, physiology, and disease. J Cell Biol. 2011; 193: 607–618. DOI: 10.1083/jcb.201012094 [PubMed: 21576390]
36. De Bock K, Mazzone M, Carmeliet P. Antiangiogenic therapy, hypoxia, and metastasis: risky liaisons, or not? Nat Rev Clin Oncol. 2011; 8: 393–404. DOI: 10.1038/nrclinonc.2011.83 [PubMed: 21629216]

37. Steeg PS. Tumor metastasis: mechanistic insights and clinical challenges. Nat Med. 2006; 12: 895–904. DOI: 10.1038/nm1469 [PubMed: 16892035]
38. Hong CS, et al. LB100, a small molecule inhibitor of PP2A with potent chemo- and radio-sensitizing potential. Cancer Biol Ther. 2015; 16: 821–833. DOI: 10.1080/15384047.2015.1040961 [PubMed: 25897893]
39. Chung V, et al. Safety, Tolerability, and Preliminary Activity of LB-100, an Inhibitor of Protein Phosphatase 2A, in Patients with Relapsed Solid Tumors: An Open-Label, Dose Escalation, First-in-Human, Phase I Trial. Clin Cancer Res. 2017; 23: 3277–3284. DOI: 10.1158/1078-0432.CCR-16-2299 [PubMed: 28039265]
40. <https://clinicaltrials.gov/ct2/results?cond=&term=LB-100&cntry=&state=&city=&dist=>
41. Kalucka J, et al. Quiescent Endothelial Cells Upregulate Fatty Acid beta-Oxidation for Vasculoprotection via Redox Homeostasis. Cell Metab. 2018; 28: 881–894. e813 doi: 10.1016/j.cmet.2018.07.016 [PubMed: 30146488]
42. Noseda M, et al. Notch activation induces endothelial cell cycle arrest and participates in contact inhibition: role of p21Cip1 repression. Mol Cell Biol. 2004; 24: 8813–8822. DOI: 10.1128/MCB.24.20.8813-8822.2004 [PubMed: 15456857]
43. Mazzone M, et al. Heterozygous deficiency of PHD2 restores tumor oxygenation and inhibits metastasis via endothelial normalization. Cell. 2009; 136: 839–851. DOI: 10.1016/j.cell.2009.01.020 [PubMed: 19217150]
44. Scortegagna M, et al. HIF-2alpha regulates murine hematopoietic development in an erythropoietin-dependent manner. Blood. 2005; 105: 3133–3140. DOI: 10.1182/blood-2004-05-1695 [PubMed: 15626745]
45. Scortegagna M, Morris MA, Oktay Y, Bennett M, Garcia JA. The HIF family member EPAS1/HIF-2alpha is required for normal hematopoiesis in mice. Blood. 2003; 102: 1634–1640. DOI: 10.1182/blood-2003-02-0448 [PubMed: 12750163]
46. Joseph BK, et al. Inhibition of AMP Kinase by the Protein Phosphatase 2A Heterotrimer, PP2APpp2r2d. J Biol Chem. 2015; 290: 10588–10598. DOI: 10.1074/jbc.M114.626259 [PubMed: 25694423]
47. Arriazu E, Pippa R, Odero MD. Protein Phosphatase 2A as a Therapeutic Target in Acute Myeloid Leukemia. Front Oncol. 2016; 6: 78. doi: 10.3389/fonc.2016.00078 [PubMed: 27092295]
48. Betz C, Lenard A, Belting HG, Affolter M. Cell behaviors and dynamics during angiogenesis. Development. 2016; 143: 2249–2260. DOI: 10.1242/dev.135616 [PubMed: 27381223]
49. Yun S, et al. Integrin alpha5beta1 regulates PP2A complex assembly through PDE4D in atherosclerosis. J Clin Invest. 2019; 130 doi: 10.1172/JCI127692
50. Watson EC, Grant ZL, Coultas L. Endothelial cell apoptosis in angiogenesis and vessel regression. Cell Mol Life Sci. 2017; 74: 4387–4403. DOI: 10.1007/s00018-017-2577-y [PubMed: 28646366]
51. Skuli N, et al. Endothelial HIF-2alpha regulates murine pathological angiogenesis and revascularization processes. J Clin Invest. 2012; 122: 1427–1443. DOI: 10.1172/JCI57322 [PubMed: 22426208]
52. Mudgett JS, et al. Essential role for p38alpha mitogen-activated protein kinase in placental angiogenesis. Proc Natl Acad Sci U S A. 2000; 97: 10454–10459. DOI: 10.1073/pnas.180316397 [PubMed: 10973481]
53. Ferrari G, et al. TGF-beta1 induces endothelial cell apoptosis by shifting VEGF activation of p38(MAPK) from the prosurvival p38beta to proapoptotic p38alpha. Mol Cancer Res. 2012; 10: 605–614. DOI: 10.1158/1541-7786.MCR-11-0507 [PubMed: 22522454]
54. Zarubin T, Han J. Activation and signaling of the p38 MAP kinase pathway. Cell Res. 2005; 15: 11–18. DOI: 10.1038/sj.cr.7290257 [PubMed: 15686620]
55. Casazza A, et al. Systemic and targeted delivery of semaphorin 3A inhibits tumor angiogenesis and progression in mouse tumor models. Arterioscler Thromb Vasc Biol. 2011; 31: 741–749. DOI: 10.1161/ATVBAHA.110.211920 [PubMed: 21205984]
56. Shojaei F, et al. Tumor refractoriness to anti-VEGF treatment is mediated by CD11b+Gr1+ myeloid cells. Nat Biotechnol. 2007; 25: 911–920. DOI: 10.1038/nbt1323 [PubMed: 17664940]
57. Kamba T, McDonald DM. Mechanisms of adverse effects of anti-VEGF therapy for cancer. Br J Cancer. 2007; 96: 1788–1795. DOI: 10.1038/sj.bjc.6603813 [PubMed: 17519900]

58. Carmeliet P, Jain RK. Molecular mechanisms and clinical applications of angiogenesis. Nature. 2011; 473: 298–307. DOI: 10.1038/nature10144 [PubMed: 21593862]

Europe PMC Funders Author Manuscripts

What is new?

B55α/PP2A elicits a HIF- and p38-dependent survival program during vascular remodeling that protects ECs against (oxidative) cell stress.

What are the clinical implications?

B55α/PP2A inhibitors work in a complementary manner to anti-VEGF drugs, offering an alternative in case of resistance to these therapies.

Europe PMC Funders Author Manuscripts

Europe PMC Funders Author Manuscripts

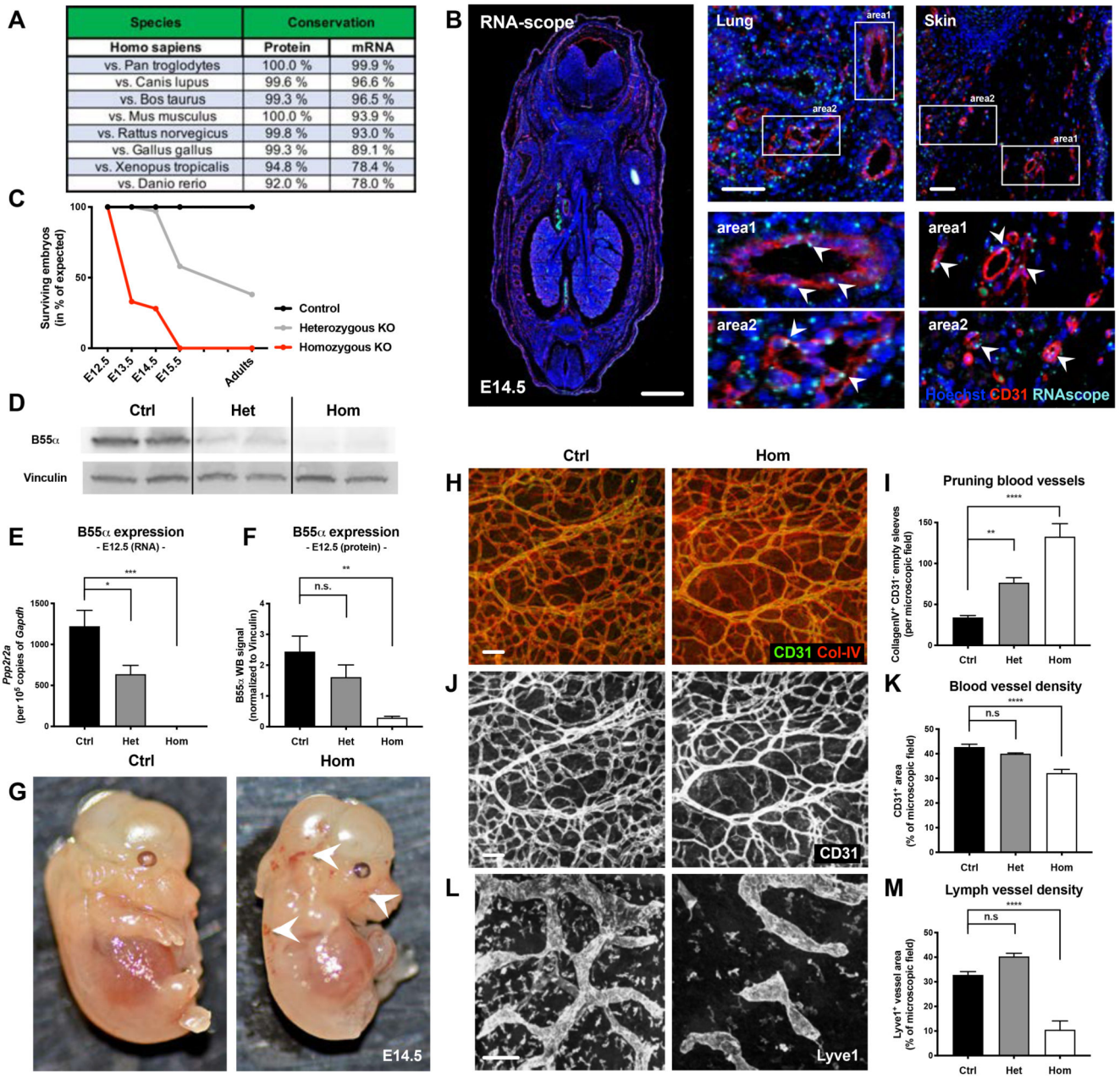

Figure 1. B55α is highly conserved among species and plays an essential role during embryonic development

(A) Analysis of B55α protein and mRNA sequences showing a high conservation between species.

(B) Expression of B55α in embryonic tissue at day 14.5 post fertilization (=E14.5) assessed by RNAscope (scale bars: 1000μm in overview and 50μm in smaller images).

(C) Ratio of surviving embryos at different stages during development in percent of the expected Mendelian ratio.

(D) Western Blot analysis of tissue samples from control, heterozygous and homozygous KO embryos at E12.5.

(E) Quantitative analysis of B55α RNA levels using qPCR in control, heterozygous and homozygous KO embryos at E12.5 (n ≥ 4 embryos per group)
(F) Quantitative analysis of B55α protein expression in tissue samples from control, heterozygous and homozygous KO embryos at E12.5 (n ≥ 5 embryos per group).
(G) Representative images of surviving littermate controls and *Ppp2r2a* Full KO embryos at embryonic stage E14.5.
(H,**J**,**L)** Representative images of embryonic skin samples from *Ppp2r2a* KO and littermate controls stained for Collagen IV and $CD31^+$ blood vessels **(J)** and $Lyve1^+$ lymph vessels **(L)** (Scale bars: 100 μm).
(I,**K**,**M)** Quantitative analysis of Collagen IV^+ / $CD31^-$ pruning blood vessels (n ≥ 6 per group) **(I)**, $CD31^+$ blood vessel area (n ≥ 3 per group) **(K)** and $Lyve1^+$ lymph vessel area (n ≥ 4 per group) **(M)** in surviving embryos at stage E14.5.
P values are *p<0,05; **p<0,001; ***p<0,001; ****p<0,0001.
Graphs show standard error of the mean (SEM).

Europe PMC Funders Author Manuscripts

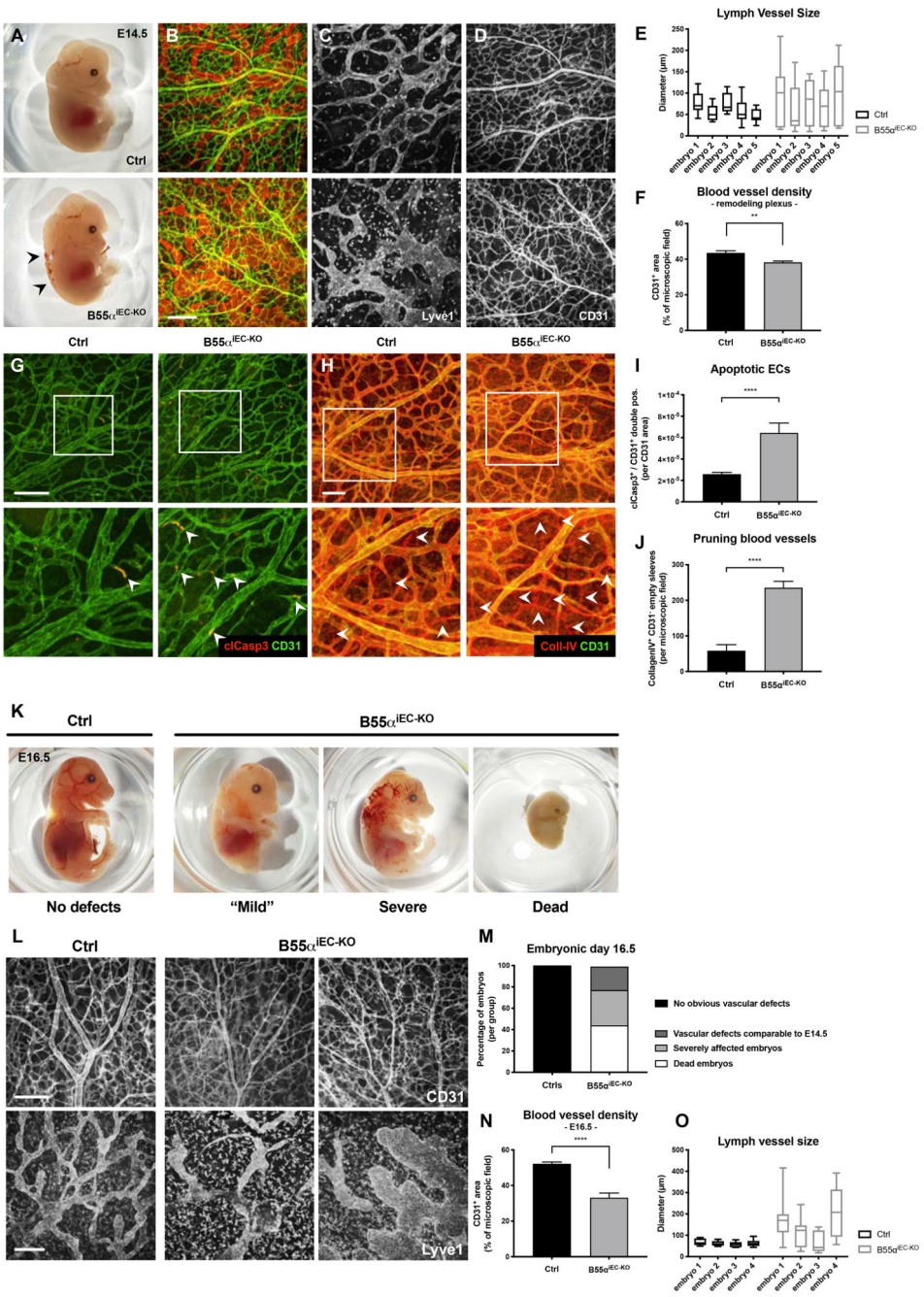

Figure 2. Endothelial loss of B55α leads to severe vascular and lymphatic defects during embryonic development resulting in embryonic lethality

(A) Representative images of E14.5 embryos lacking endothelial B55α and littermate controls. **(B-D)** Whole mount skin samples stained for lymph vessel marker Lyve1 **(C)** and the blood vessel marker CD31 (Scale bar: 200μm) **(D)**

(E,**F)** Quantitative analysis of lymph vessel diameter (n = 4 embryos per group) **(E)** and blood vessel density in the remodeling vascular plexus (n ≥ 12 embryos per group) **(F)**.

Europe PMC Funders Author Manuscripts

(G,**I)** Apoptotic ECs in the remodeling vascular plexus indicated by immunostainings against CD31 and cleaved Caspase3 (Scale bar: 100μm) **(G)** and quantitative analysis thereof **(I).**

(H,**J)** Pruning blood vessels, visualized by Co-staining of $CD31^+$ and $CD31^-$ / $CollagenIV^+$ empty sleeves (Scale bar: 100μm) **(H)** and quantitative analysis thereof (n = 4 per group) **(J).**

(K,**M)** Representative images of whole embryos at stage E16.5 showing differentially affected mutants and statistical quantifications thereof **(M)**.

(L,**N**,**O)** Representative images of embryonic skin samples stained for $CD31^+$ blood vessels and $Lyve1^+$ lymph vessels **(L)** and statistical analysis thereof (Scale bars = 200μm) **(N**,**O)** The statistical analysis was performed on 9 embryos per group for **(N)** and 4 embryos per group for **(O)**.

P values are *p<0,05; **p<0,001; ***p<0,001; ****p<0,0001.

Graphs show standard error of the mean (SEM).

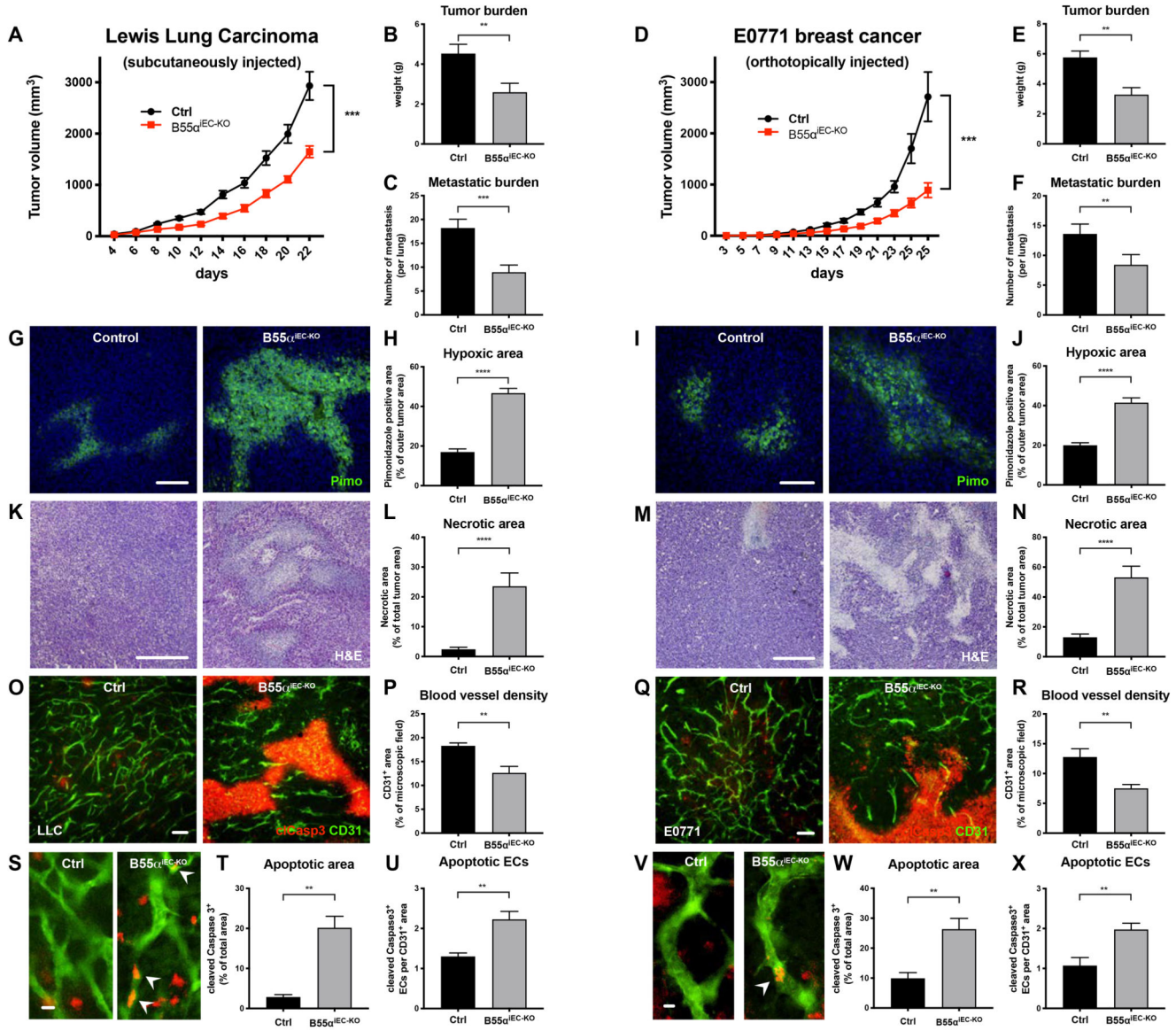

Figure 3. EC specific deletion of B55α leads to a strong delay in tumor growth lung metastasis, due to a reduced number of blood vessels.

(A-F) Tumor progression after EC specific deletion of *Ppp2r2a* following the subcutaneous injection of LLC cancer cells, showing delayed tumor growth, a smaller tumor burden and less lung metastasis in mutant mice (n ≥ 8 per group) **(a-c)** and orthotopically injected E0771 breast cancer cells (n ≥ 9 per group) **(D-F)**.

(G-J) Representative images and quantifications of hypoxic areas in LLC **(G**,**H)** and E0771 tumors (n ≥ 8 per group, Scale bars = 100μm) **(I**,**J)**.

(K-N) Representative images and quantifications and of necrotic areas in LLC **(K**,**L)** and E0771 tumors (n ≥ 7 per group, Scale bars = 400μm) **(M**,**N)**

(O-T) 70μm thick cryosections of LLC **(O**,**S)** and E0771 **(Q**,**V)** tumors stained for CD31^{+} blood vessels and the apoptosis marker cleaved Caspase3 and statistical analysis of blood

vessel density **(P**,**R)**, total area of apoptotic (tumor) areas **(T**,**W)** and cleaved Caspase3^{+} ECs **(U**,**X)** (n ≥ per group, Scale bars **(O**,**Q)** = 100μm; Scale bars **(S**,**V)** = 10μm).
P values are *p<0,05; **p<0,001; ***p<0,001; ****p<0,0001.
Graphs show standard error of the mean (SEM).

Europe PMC Funders Author Manuscripts

Europe PMC Funders Author Manuscripts

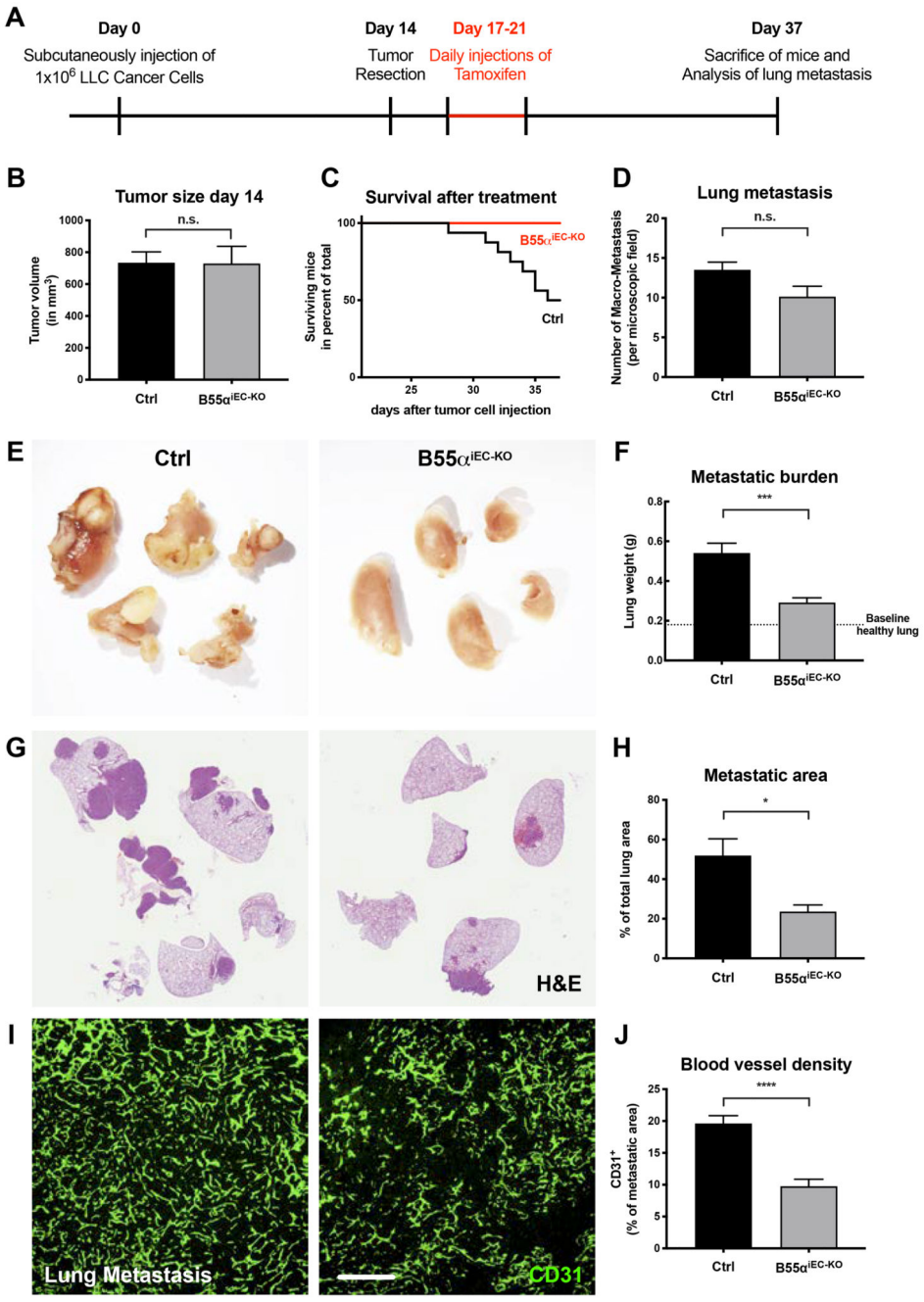

Figure 4. Deletion of B55α in the endothelium after removal of the main tumor delays metastatic growth and prolongs the survival of mutant mice.

(A) Schematic layout of the depicted experiment.

(B) Quantitative analysis of tumor size at the time point of tumor resection showing no differences between littermate controls and non-tamoxifen injected mutant mice.

(C) Quantitative analysis showing the survival rates of littermate controls and mutant mice after main tumor resection and subsequent tamoxifen induced depletion of endothelial *Ppp2r2a*.

Europe PMC Funders Author Manuscripts

(D) Quantitative analysis of the number of lung metastasis at the end stage of the experiment.
(E,**F)** Representative overview images showing metastatic lungs from tamoxifen treated littermate controls and mutant mice **(E)** and the quantitative analysis thereof **(F)**.
(G,**H)** Representative images showing H&E stained lungs showing healthy lung areas and the dense metastatic areas in littermate controls and mutant mice **(G)** and the quantitative analysis thereof **(H)**.
(I,**J)** Representative images showing the vasculature within lung metastasis in littermate controls and mutant mice (Scale bar = 200μm) **(I)** and the quantitative analysis thereof **(J)**.
The statistical analysis was performed on a minimum of 8 animals per group.
P values are *p<0,05; **p<0,001; ***p<0,001; ****p<0,0001.
Graphs show standard error of the mean (SEM).

Europe PMC Funders Author Manuscripts

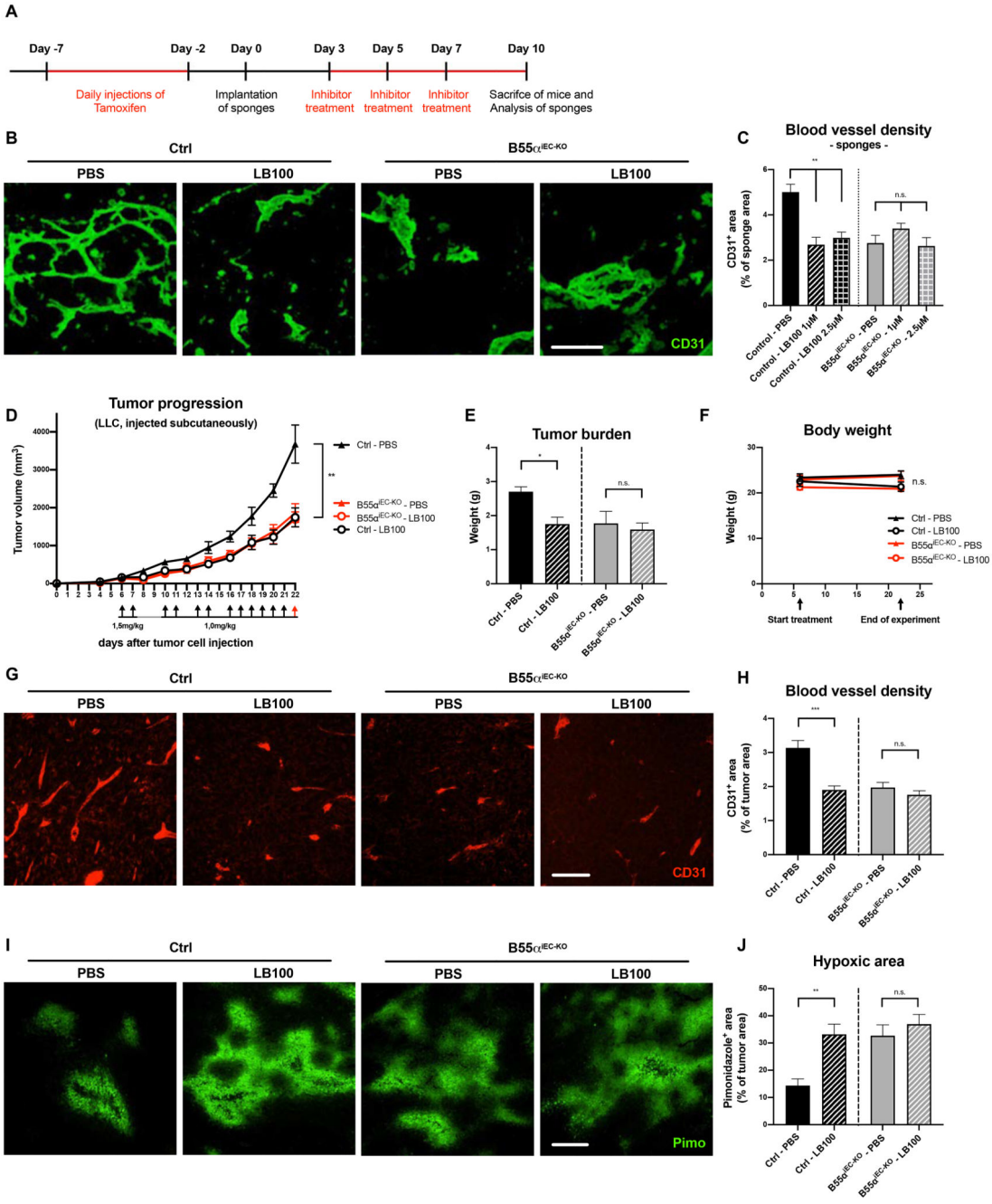

Figure 5. Chemical inhibition of the PP2A phosphatase induces blood vessel pruning and delays tumor progression *in vivo*.

(A) Schematic representation and time frame of the sponge implantation assay shown in (B,C)

(B, C) Representative images of sponges stained for $CD31^+$ blood vessels (Scale bar: 100µm)

(B) and quantitative analysis thereof ($n \geq 7$ per group) **(C)**.

(D-F) Subcutaneous LLC tumor growth **(D)** and final tumor burden **(E)** after EC-specific deletion of Ppp2r2a or systemic LB100 treatment (alone and in combination), showing a similar delay in cancer progression when compared to untreated wildtype mice, albeit no significant changes in total body weight **(F)**.
(G, H) 6μm thin paraffin sections of tumor samples stained for CD31+ blood vessels (Scale bars: 100μm) **(G)** and statistical analysis of blood vessel density **(H)**.
(I, J) Representative images (Scale bars: 200μm) **(I)** and quantifications **(J)** of pimonidazole-positive tumor areas, indicating hypoxic regions.
P values are *p<0,05; **p<0,001; n ≥ 4 mice per condition in A-G.
Graphs show standard error of the mean (SEM).

Europe PMC Funders Author Manuscripts

Europe PMC Funders Author Manuscripts

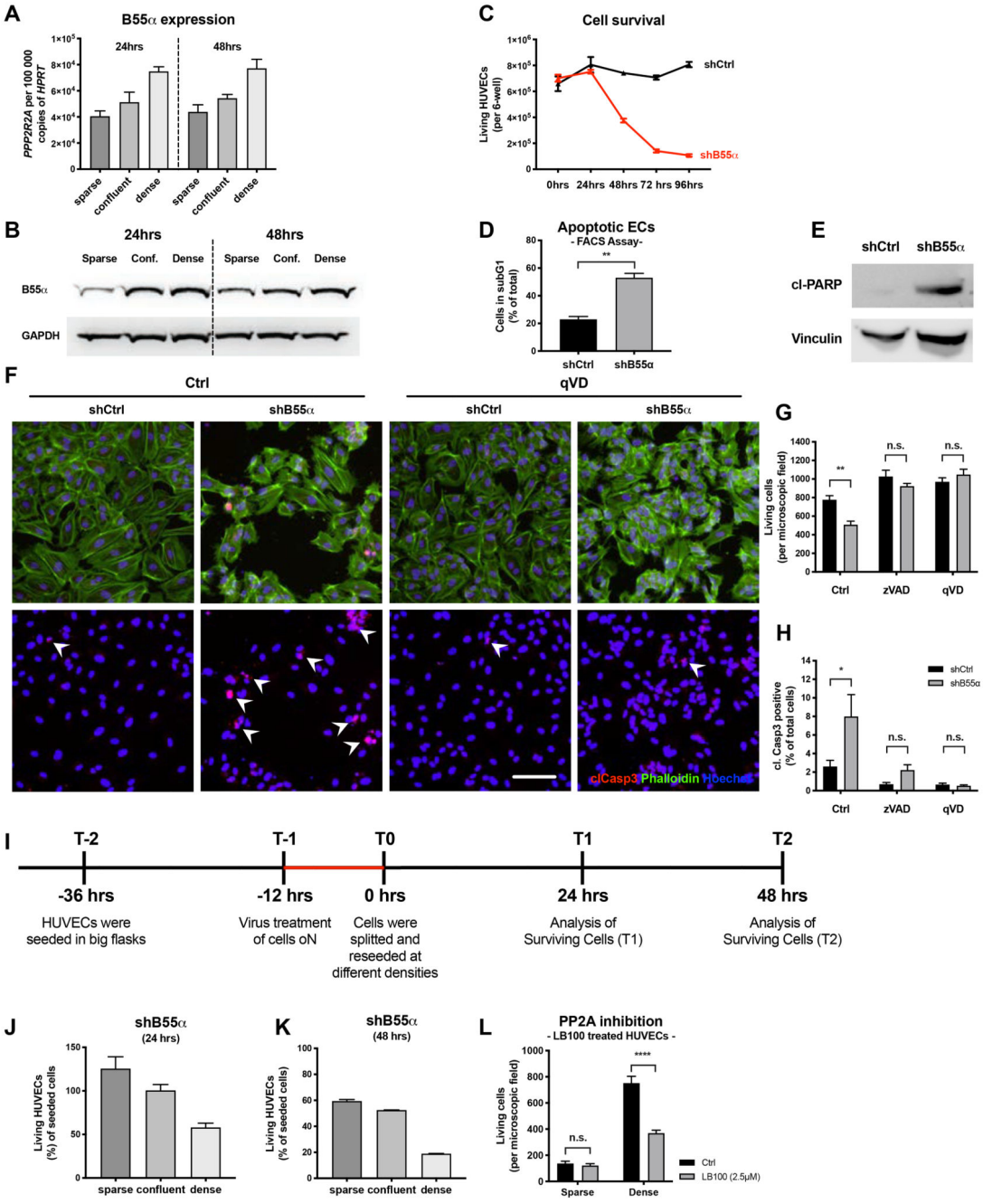

Figure 6. ***In vitro*, B55alpha is upregulated in a density dependent manner and needed to protect HUVECs against activation of the endogenous apoptosis pathway.**

(A,**B)** Analysis of B55α expression in HUVECs cultured at different densities, showing an upregulation in a density dependent manner on RNA **(A)** and protein level **(B)**.

(C-E) Analysis of living ECs after KD of B55α showing a drastic reduction of living HUVECs

(C) and simultaneously an upregulation of apoptosis markers as analyzed by FACS **(C)** and WB **(E)**.

(F-H) Immunostainings of B55α-KD HUVECs treated with pan-Caspase inhibitors (qVD or zVAD) for Phalloiding (green), the apoptosis marker cleaved Caspase3 (red) and Hoechst (Scale bar: 100μm) **(F)** and quantitative analysis thereof **(G-H)**.
(I) Schematic representation and timeline of the experiments depicted in **(J)** and **(K)**.
(J,**K)** Analysis of living HUVECs after KD of B55α showing a stronger induction of apoptosis in dense HUVECs, mimicking a more quiescent-like phenotype.
(L) Results showing that chemical inhibition of PP2A phosphatase activity recapitulates the reduction of living HUVECs in dense conditions, while barely affecting sparse HUVECs.
All statistical analysis was conducted on a minimum of 3 samples per group and are representative from 3 independent repetitions.
P values are *p<0,05; **p<0,001; ***p<0,001; ****p<0,0001.
Graphs show standard error of the mean (SEM).

Europe PMC Funders Author Manuscripts

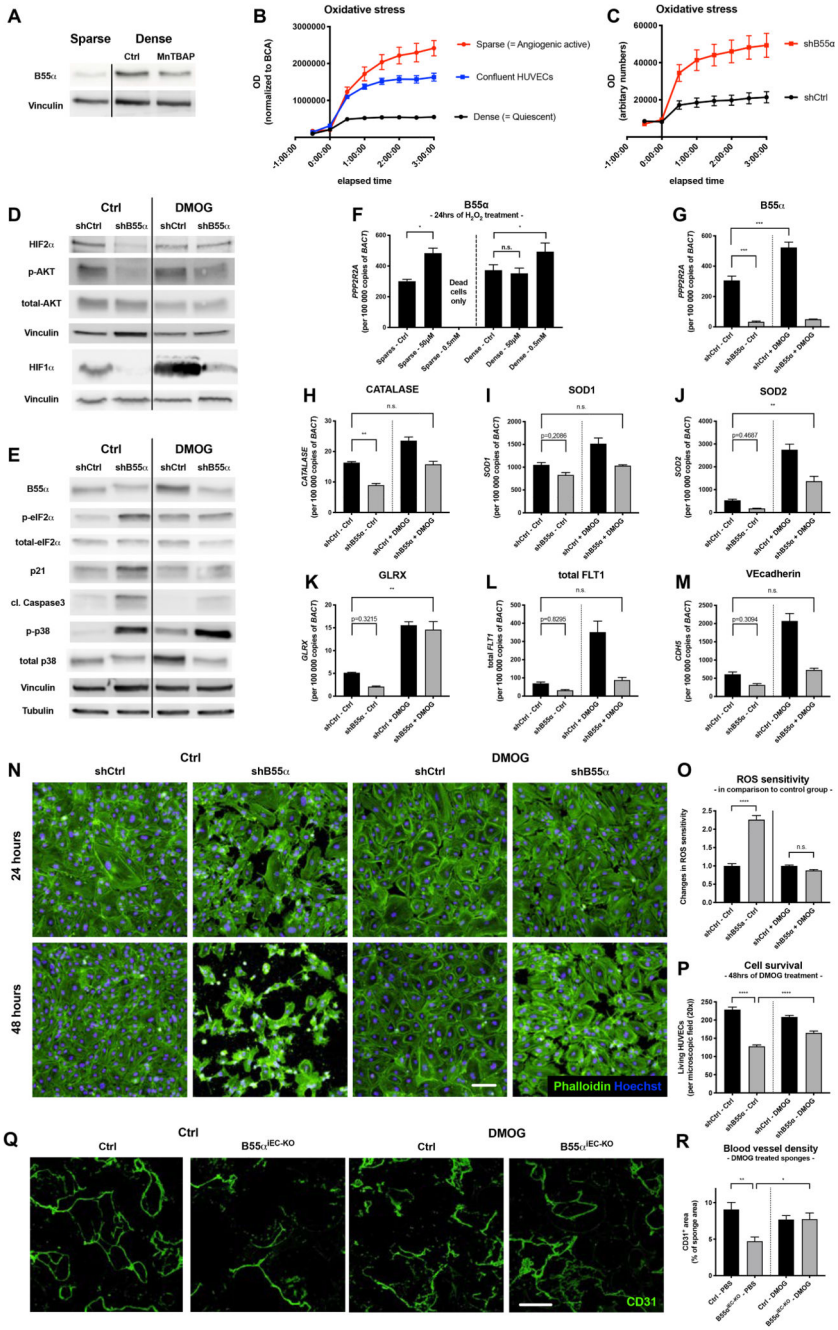

Figure 7. B55α induces cell protection against ROS and cell stress partially in a PHD dependent manner

(A) WBs showing that the upregulation of B55α under dense conditions can be partially inhibited with the ROS scavenger MnTBAP

(B) ROS sensitivity assay analyzing the differential effects of H_2O_2-induced ROS on sparse, confluent and dense HUVECs.

(C) Analysis of ROS sensitivity in qVD treated HUVECs showing the differential response of B55α-KD HUVECs to H_2O_2 induced ROS-stress under dense conditions.

(D,**E)** WB analysis of different proteins indicating increased cell stress (such as p-eIF2α and p21), proteins involved in counteracting cell stress (HIF1α, HIF2α, p-AKT) and the apoptosis marker cleaved Caspase3 in B55α-KD and DMOG treated HUVECs.
(F-M) qPCR-based expression analysis of B55α **(F**,**G)**, genes counteracting ROS (Catalase **(H)**, SOD1 **(I)**, SOD2 **(J)**, GLRX **(K))** and EC maturation markers such as total Vegfr1 **(L)**, and VEcadherin **(M)**.
(N-P) Staining of Phalloidin and Hoechst in DMOG treated B55α-KD and control HUVECs (Scale bar: 100μm) **(N)** and quantification of the increased resistance to H_2O_2 **(O)** and cell survival **(P)**.
(Q,**R)** Representative images of sponges stained for $CD31^+$ blood vessels (Scale bar: 300μm)
(Q) and quantification thereof (n = 6 per group) **(R)**.
P values are *p<0,05; **p<0,001; ***p<0,001; ****p<0,0001.
Graphs show standard error of the mean (SEM).

Europe PMC Funders Author Manuscripts

Europe PMC Funders Author Manuscripts

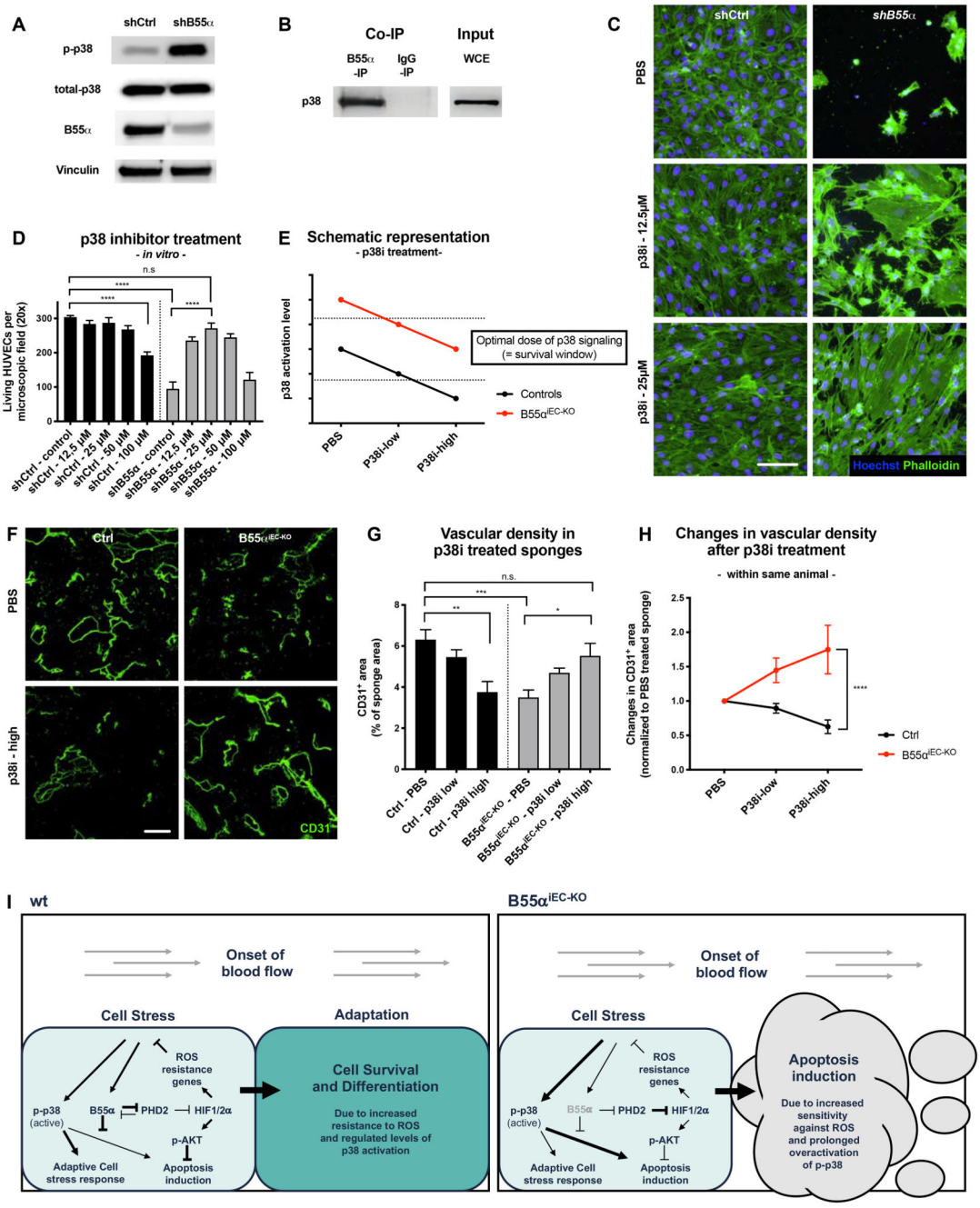

Figure 8. B55α dephosphorylates p-p38 and thereby inhibits its prolonged and apoptosis inducing activity

(A) WB analysis showing that KD of B55α leads to elevated levels of activated p-p38, while not affecting the total levels thereof.

(B) Co-IP experiments performed in dense HUVECs showing a direct interaction between B55α and p38.

(C,**D)** Cultured Ctrl and B55α-KD HUVECs stained for Phalloidin and Hoechst (Scale bar 100μm) **(C)** showing a dose dependent rescue of cell numbers by inhibition of p38 in B55α-KD, but not in control cells (D).

(E) Schematic representation of p38 control on EC apoptosis, explaining the results of the experiments depicted in **(A)** and **(D)**.

(F-H) Immunostainings for $CD31^+$ blood vessels of implanted sponges derived from control and $B55\alpha^{iEC\text{-}KO}$ mice (Scale bar: 300μm) **(F)**, showing a dose dependent improvement of vessel density after p38 inhibitor treatment in $B55\alpha^{iEC\text{-}KO}$ but not in control mice **(G**,**H)**.

(I) Graphical abstract summarizing our findings and the proposed mechanism

P values are *p<0,05; **p<0,001; ***p<0,001; ****p<0,0001.

Graphs show standard error of the mean (SEM).

Europe PMC Funders Author Manuscripts